

repeatedly quenched until the same current was obtained to within ± 50 amperes on four successive quenches. Then the energy into and out of the magnet was carefully measured^{3,4}. This utilized a standard 3.2T and 4.4T cycle at several different ramp rates. The magnet temperature was then reduced 0.5K to 1K, and the quenching continued until the current became constant. The magnet was then warmed to 4.2K and a curve was taken of quench current versus ramp rate.

A Morgan coil was placed in the aperture and the sextupole signal (β_0) was measured as a function of angle for a given powering cycle of 800 gauss/sec from 0.440T up to 4.4T and down. From these data, the β_0 magnetization widths are obtained, then β_0 was measured up to quench. There was also a measurement of β_0 as a function of a) temperature, b) ramp rate, dB/dt, c) field, B, and d) very low current behavior of β_0 with a very stable battery power supply. It was at this point that special experiments, such as the strain gauge measurements of the deflection of the coils, were performed. Then a rotating Morgan coil was placed in the aperture and harmonics were measured as a function of excitation current, ramp rate, and powering sequence. Usually as a final check, the magnet was quenched a few times to see if it still trained before the model was warmed to 77K and the DC harmonics were measured again. This procedure was repeated at 300K.

Results and Conclusions

Quench Performance

Quench performance of the models is summarized in Table II. Typical quench data are contained in Figures 1, 2, and 3. Figures 1 and 2 show load lines, cable characteristics at two temperatures and a typical quench sequence for a quadrupole and dipole. Figure 3 shows training curves for three of the model dipoles. Figure 4 shows quench sensitivity to ramp rate. Because of the large number of models and the extensive data taken, only the more significant results will be discussed.

TABLE II
QUENCH SUMMARY

Number	Critical Current ^a (kA) Cable (kA)	High Quench (kA) 4.2K	# Quenches to 95.7%	# Quenches 99% +	Highest Quench (kA) at any Temperature	ΔI_Q $\Delta(B/dt)$ 0 = 1600/sec
TS02509	6.8	6.7	2	1	7.0	0
TS02511	5.37	5.55	1	2	6.75	0
TS02512	5.37	5.50	1	2	6.10	0
RA1001	5.98	5.87	0	13	6.08	42
RA1001-R	5.95					
RB1001	6.18	6.05	8	23	6.05	
RB1001-R	6.18	6.21	3	5	6.67	25
RC1001	6.18	6.0	10(23) ^b	76(43) ^b	6.0	562
RC1001-R	6.18	6.18	2	4	6.38	313
RB1001-S	6.18	6.09	22	31	6.73	562
RB1001-S	6.18	6.1				
RF1001	5.52	5.42	5	8	6.02	94
RF1001	5.52	5.4	0	Never reached	5.44	99
RC1001-S	6.18	6.08	5	12	6.49	189
RI1001	5.94	6.11	9	18	6.1	31
RJ1001	6.05	5.98	7	10	6.57	125

^a The quench number in parenthesis includes those quenches that occurred before a bad splice was discovered and repaired.
^b The current at the intersection of the 2T high field point in the windings at the operating temperature with an effective cable resistivity of $2 \times 10^{-12} \Omega\text{-cm}$ is used as the definition of the winding's critical current. The percentages are based on that current value.

R = Aluminum Outside Collar Clamps
 S = Special Deflection Cause Test

Collar Strength The higher current capacity cable or testing of the models at temperatures below 4.2K have made it possible to exceed the mechanical limits of the Tevatron collars. The NbTi dipole models with such collars could not be made to exceed a current of 6.0kA, even if the cable short sample current was raised by lowering the bath temperature below 4.2K. This limitation has been attributed to outward flexing of the collars at the midplane. To test this

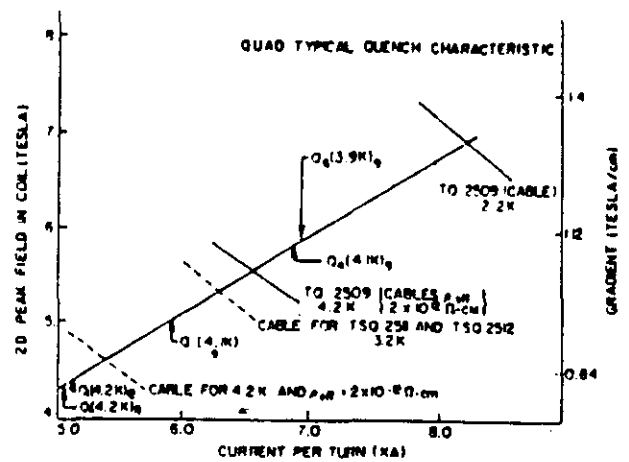


Figure 1

The critical current as a function of magnetic field is plotted for two different cables and three different field temperature intersect the two dimensional high field load line for the Tevatron quadrupoles. The first quench (superconducting to normal transition) for TQ11 (TSQ2511) is denoted by Q_1 (4.2K)₁₁ for a temperature of 4.2K. The central gradient is given on the right hand scale.

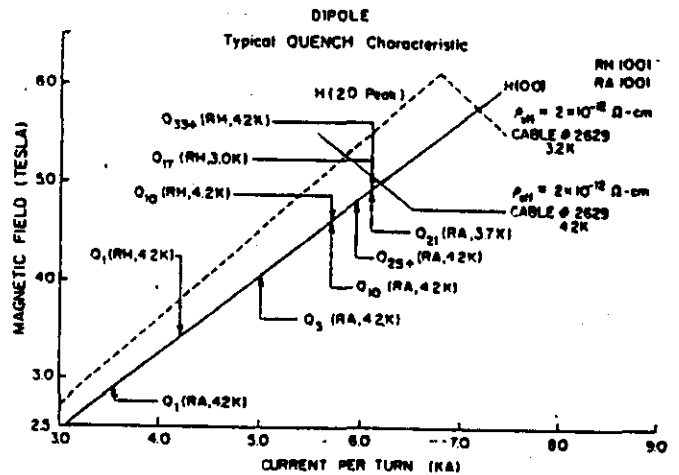


Figure 2

The central field load line (solid) is plotted with the critical current at an equivalent cable resistivity of $2 \times 10^{-12} \Omega\text{-cm}$, short sample, for two different cable temperatures, 4.2K and 3.2K. The designation for quench number 3 for magnet RA1001 at 4.2K is Q_3 (RA, 4.2K).

hypothesis, two inch thick aluminum rings were bolted around two of the collared coils (RB and RC). When these magnets were retested, they easily reached their short sample limit and passed beyond the 6.0kA limit to greater than 6.5kA at reduced temperatures. Mechanical motion of the collar system was also studied using a strain gauge fixture attached to the collared coil. Results indicated a radial displacement of 0.0106 ± 0.0015 inches at the midplane, consistent with collar stress calculations at 6kA. Model RJ, which used a NbTiTa alloy cable, however, operated at low temperature to currents above 6.5kA. The NbTiTa has a twenty-five percent higher low temperature performance than NbTi and was therefore believed not to be as motion sensitive.

Helium Irrigation Magnet models were built with standard Tevatron helium irrigation spacers between

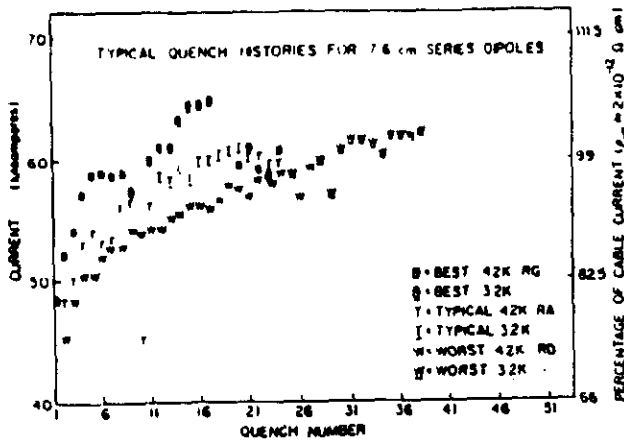


Figure 3

The quench current (or % of cable current attainable on the magnet load line) at 4.2K is plotted against quench number. The most rapidly training case, the typical case, and the slowest case are shown.

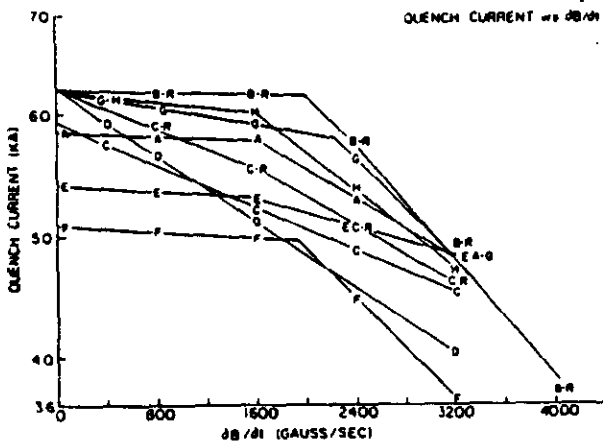


Figure 4

Figure 4 gives the maximum quench current for a given model as a function of ramp rate (actual data shown by symbols).

inner and outer coils (intermediate banding) or with one of two simpler schemes that severely restrict helium circulation. In the interest of reducing fabrication cost, the latter systems use perforated or solid Kapton sheet rather than the complex helical epoxy fiberglass spacers. The perforated Kapton restricts the helium between coils to radial flow only. The solid Kapton eliminates even radial flow. The models, both quadrupole and dipole, using perforated Kapton or solid Kapton intermediate banding show no significant differences in quench performance at SSC ramp rate as compared to the standard helical system. As shown in Figure 4, the quench performance of the dipole model RD with the solid Kapton deteriorates rapidly with increasing ramp rate, nevertheless there was little ($\leq 1\%$) deterioration at even double the SSC rate.

High field point The highest field in the coil is in the end turns and is calculated to be about 15% above the central field. The quench data, however, show that the maximum current appears to be limited by the high field point in the middle of the coil body of the magnet, the "2D high field point". The 2D high field point is only 7% above the central field. A subset of models that is clearly not limited by

collars (RA, RB-R, RC-R, RE, RF, RH, and RJ), achieve maximum currents at the 2D limit within the variation of the cable short sample current ($\pm 2\%$). See Table II. This holds true for the quadrupoles as well as the dipoles. Although this observation is not well understood, several explanations are plausible, i.e., current sharing among the strands in the end turns, dependence of I_c on the angle between cable and field.

Copper to superconductor ratio Models were made with cable having three Cu/SC ratios: 1.8, 1.5, and 1.3. Figure 3 illustrates the comparison between models with 1.3 and 1.8 ratios. Both cables have short sample limits of about 6.0kA. Beyond the first few quenches RD (1.3) trains more slowly than RA (1.8). Model RJ (Cu/SC=1.5) has nearly the same quench behavior as the magnets with Cu/SC=1.8. This data suggests that the margin for stability, near short sample, decreases rapidly below a Cu/SC ratio of 1.5.

Coil loading and collar material All of the models were assembled with standard Tevatron room temperature preload. A dipole model made of standard Tevatron cable with a typical short sample of 5300 Amps reaches 95% of maximum current in just a few quenches (≤ 5). The models with a cable short sample around 6000 Amps require eight or more quenches to reach 95%. To study the use of aluminum collars, a model was made (RG) with aluminum collars identical in size and shape to the stainless steel Tevatron collars. Since the 6061 (T6) aluminum alloy collars were substantially weaker than the stainless collars, the aluminum collar support rings described earlier were added. The aluminum collars shrink more than the coil and increase preload on cooling. One result of increased coil loading is clear in the steeper quench curve for RG shown in Figure 3.

Quench sensitivity to ramp rate The quench current as a function of ramp rate is given in Figure 4. The initial slope of the dipole models is given in Table II. There appears to be two distinct regions for most of the models. The region below 1.6 kilogauss/sec is primarily governed by the strand and filament characteristics plus cooling. Above 2.4 kilogauss/sec, where most of the conductor is coupled, normal eddy currents are a dominant factor. Models RC and RD have sharply steeper slopes. These models have larger losses in the winding and are poorly irrigated (Kapton, and punched Kapton intermediate banding) and temperature goes up. RG1001 also has perforated Kapton, but due to the higher clamping; the losses are lower, therefore, the coil temperature is less.

Energy Loss Measurements

The magnet models have had extensive energy-in minus energy-out measurements¹ made during various ramp rate and clamping conditions (i.e., with stainless steel collars plus aluminum retaining rings or without, or aluminum collars etc.). Figure 5 shows the loss per cycle for various models as a function of ramp rate for a 0 to 3.2T to 0 cycle. Figure 5 also includes a curve for a Lawrence Berkeley four layer dipole (symbol LBL) which was constructed of standard Tevatron conductor. This data has been normalized to the same average magnetic field winding volume as the 7.6cm aperture dipoles. The degree of rate sensitivity is indicative of higher clamping forces and therefore lower interstrand resistance². The losses on at 4.25T cycle are 1.3 times those on a 3.2T cycle.

The shape of the loss curve is to some extent a measure of how stiff the winding and supporting

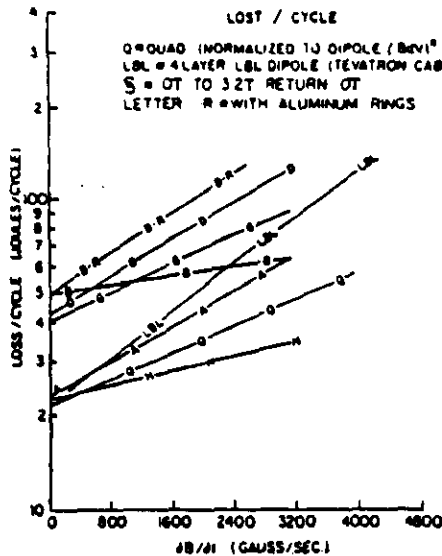


Figure 5

In Figure 5; the loss/cycle is shown for various model magnets, both dipoles and quadrupoles (which have been normalized to the same average magnetic field winding volume as the dipoles).

structure is⁶. The shape of the X axis of the Ein-Eout curve for a given measurement may be expressed as $-C(I-I_0)^2$. Table III lists the constants of this empirical equation when fitted to the Ein-Eout curves. The smaller values of C indicate a stiffer structure and these magnets tended to train less and reach higher ultimate quench currents (by reduced temperature). The significance of I_0 is not clear.

TABLE III

Shape of the Ein-Eout Curves
 $=C(I-I_0)^2$

Model Desig.	$C(\frac{\text{volt-sec}}{\text{KA}^2})$	I_0
Quads	0.046	1.9
Dipoles		
RA - RF	0.111	1.4
RB-R & RC-R	0.08	1.4
RH1001	0.14	1.4
RJ1001	0.096	1.4
RG1001	0.066	1.4

Magnet field characteristics

In Table IV, the transfer co-efficient for RG1001 and 3θ are given as a function of model magnet current.

The ratio of the difference in B_z (sextupole) on the ramp up and B_z on the ramp down for RD1001, which has 19 micron filament cable to their difference for RA1001 with 9 micron, high critical current filament cable, is 2.5 ± 2 . This is in agreement with the ratio's of the critical currents and filament diameter of each. The ratio of the sextupole widths for RE1001 and RA1001, both of which have 9 micron filaments, is 1.36 ± 2 , which is in agreement with the critical

TABLE IV
 Magnetic field and sextupole as
 a function of Magnet Current
 Model RG1001

Current/Turn(A)	1000	2000	3000	4000	5000
B_z Tesla	.015	1.619	2.420	3.223	4.026
$B_z(2θ)$ (1/Lm ²)	0.3	16.2	16.0	16.1	20.3
Transfer (Amps) Param.	0.150	0.097	0.086	0.083	0.075

current values. These data were obtained by integrating 3θ voltage on a peak value angle (stationary coil, changing field).

High field option

The 10T, 10kA/turn models represent a much longer term and more complex series with a new coolant scheme, (1.8K) as well as much higher forces and material (superconducting ternary)⁷ development requirements. The low temperature performance of RJ1001 may offer some insight into possible NbTiTa performance and it's operational characteristics as a multi-kiloampere magnet conductor. RJ1001 will also be operated in the superfluid rig to gain insight in the new coolant scheme.

Future Plans

The 7.6cm model program has been a rich source of data for understanding the performance of superconducting magnets. The current program will probably continue for another year. Many areas of study remain, including conductor characteristics, coil clamping, persistent current corrections and insulation schemes. Gradually, the focus will shift to 5cm aperture models which will evolve into the final SSC design. As experience is gained with the half and full scale model programs that are proceeding in parallel, the short model program will provide for quick turn-around tests of magnet refinements. The dipole collared coil is the heart of the SSC and it's most costly single component. The investment made in model programs such as described here can have an enormous impact on the success of the SSC project.

References

1. Fermilab TEV Program, "Superconducting Magnet Ring". Fermilab Report, May, 1977.
2. M. Tigner, 'Superconducting Super Collider' Reference Designs Study for U. S. Department of Energy. Report of the Reference Designs Study Group, May 8, 1984.
3. A. D. McInturff, W. E. Fowler, K. Ishibashi, M. Kuchnir, R. A. Lundy, and A. V. Tollestrup, IEEE Transactions on Nuclear Science, Vol. NS-30, No. 4, p. 3393, Aug., 1983.
4. M. Kuchnir, Fermilab Tech Note, 'Interstrand Resistance in Cables'.
5. M. N. Wilson, CRYOGENICS, June, p. 361, (1973).
6. A. D. McInturff and D. Gross, IEEE Transactions on Nuclear Science, Vol NS-28, No. 3, p. 3211, June, 1981.